The International Journal of Cardiovascular Imaging (2019) 35:2029–2036
https://doi.org/10.1007/s10554-019-01664-z

ORIGINAL PAPER

Aortic roots assessment by an automated three-dimensional transesophageal echocardiography: an intra-individual comparison

Minghui Zhang[1] · **Linyuan Wan**[1] · **Kun Liu**[2] · **Weichun Wu**[1] · **Hui Li**[1] · **Yuan Wang**[3] · **Bin Lu**[2] · **Hao Wang**[1]

Received: 9 February 2019 / Accepted: 3 July 2019 / Published online: 11 July 2019

Abstract

To evaluate the accuracy, reproducibility, and transcatheter heart valve (THV) sizing efficiency of an automated 3-dimensional transesophageal echocardiographic (3D-TEE) post-processing software in the assessments of aortic roots, intra-individually compared with multidetector computed tomography (MDCT). We prospectively studied 67 patients with normal aortic roots. We measured diameters of aortic annulus (AA), sinus of Valsalva (SOV), and sino-tubular junction (STJ) by full-automated and semi-automated methods using 3D-TEE datasets, then compared them to corresponding transthoracic echocardiography and MDCT values. THV sizes were chosen based on echocardiography and MDCT measurements according to recommended criterion. Taking MDCT planimetered diameters as reference, the full-automated (r: 0.4745–0.8792) and semi-automated (r: 0.6647–0.8805) 3D-TEE measurements were linearly correlated ($p < 0.0001$). The average differences between semi-automated or full-automated measurements and reference were 0.3 mm or 1.3 mm for AA, −1.9 mm or −0.5 mm for SOV, and −0.1 mm or 1.9 mm for STJ, respectively. The intra-class correlation coefficients of semi-automated method were 0.79–0.96 (intra-observer) and 0.75–0.92 (inter-observer). THV sizing by semi-automated measurements using echocardiographic criteria was larger than that by MDCT measurements using MDCT criteria ($p < 0.0001$) but equivalent ($p > 0.05$) if both using MDCT standards. The new automated 3D-TEE software allows modeling and quantifying aortic roots with high reproducibility. Measurements by the semi-automated method closely approximate and well correlate with the corresponding MDCT, thus THV sizing by this modeled 3D-TEE measurements should adopt recommended MDCT criteria but not echocardiographic criteria. The full-automated 3D-TEE segmentations are yet immature. (Semi-automated assessMent of Aortic Roots by Three-dimensional transEsophageal echocaRdiography [SMARTER], NCT02724709)

Keywords Three-dimensional transesophageal echocardiography · Multidetector computed tomography · Transcatheter aortic valve replacement · Automated measurement

Introduction

Although the field of transcatheter aortic valve replacement (TAVR) is continuously expanding in western countries, uptake of this treatment in Asia has been slow [1]. A reason is that anatomic considerations of the Asian population, such as smaller aorta size, high prevalence of bicuspid aortic valves, and low coronary ostia, might raise more concerns about procedural safety and complication risks. Incorrect valve selection has been proven to be the principle cause of adverse effects of TAVR. The key aspect before selecting a prosthetic transcatheter heart valve (THV) is accurate aortic annulus definition to decide the model and sizing. While several noninvasive imaging modalities are available for aortic assessment, the two most commonly utilized techniques include echocardiography and multidetector computed

---

Electronic supplementary material The online version of this article (https://doi.org/10.1007/s10554-019-01664-z) contains supplementary material, which is available to authorized users.

✉ Hao Wang
fwwangh@163.com

[1] Department of Echocardiography, Fuwai Hospital, Chinese Academy of Medical Sciences and Peking Union Medical College, National Center for Cardiovascular Diseases, 167 Beilishi Road, Beijing 100037, China

[2] Department of Radiologic Imaging, Fuwai Hospital, Chinese Academy of Medical Sciences and Peking Union Medical College, National Center for Cardiovascular Diseases, 167 Beilishi Road, Beijing 100037, China

[3] Department of Cardiology, Fuwai Hospital, Chinese Academy of Medical Sciences and Peking Union Medical College, National Center for Cardiovascular Diseases, 167 Beilishi Road, Beijing 100037, China

tomography (MDCT) [2–6]. Two-dimensional (2D) transthoracic echocardiography (TTE), even transesophageal echocardiography (TEE), is believed to underestimate the maximal annulus diameter. Three-dimensional (3D) TTE and TEE enable 3D observation of morphological information of the aortic root, but at the expense of frame resolution [2–6]. Gradually, MDCT becomes the mainstay of aortic imaging due to its higher spatial resolution and 3D compatibility, whose dataset can be easily manipulated for multiplanar reconstruction, 3D printing and virtual reality devices [7].

At this moment, a specialized TEE reconstruction software is available, which can automatically configure a geometric model of the aortic root from regular 3D-TEE images and perform a quantitative analysis of these structures. However, the accuracy of this method compared with the standard imaging techniques has not been yet evaluated by a prospective and intra-individual comparison study [8, 9].

The aim of this study was to prospectively assess the ability of this novel automated quantitative modeling of the aortic root from 3D-TEE data, and to compare the measures by this new modeled 3D-TEE with the aortic geometry obtained by current 2D-TTE, 2D-TEE and MDCT.

Materials and methods

Population

Patients were from a registered single-center clinical trial (Semi-automated assessMent of Aortic Roots by Three-dimensional transesophageal echocaRdiography [SMARTER], NCT02724709). Patients with theoretically normal aortic valves and roots were consecutively enrolled, who were clinically indicated for both TEE and MDCT mainly due to atrial fibrillation or patent foramen ovale. Our inclusion criteria were: (i) both genders, 18–75 years old, (ii) no contraindications for either TEE or cardiac CT angiography, like dysphagia and iodine allergy, (iii) written consent was obtained. Our exclusion criteria were: (i) known valvular heart disease or valves surgery, (ii) signs of angina, old myocardial infarction, or post-operation of percutaneous coronary intervention, (iii) implantation of peacemakers, occluders or other metal devices, (iv) severe cardiomyopathy, and (v) cardiac functional insufficiency (NYHA III or IV). All patients underwent 2D-TTE, 2D/3D-TEE, and MDCT examinations within 2 weeks as a procedure during March to July 2016. This study protocol was approved by the institutional review board of our hospital.

Echocardiography

2D-TTE and 2D/3D-TEE were performed by experienced echocardiographers (WW and HW) using standard echocardiography equipment (ACUSON SC2000 with 4V1c probe for TTE and Z6Ms probe for TEE, Siemens Healthineers). Images of over five cardiac cycles were recorded (Videos 1, 2). The diameters of aortic annulus (AA), sinus of Valsalva (SOV), and sino-tubular junction (STJ), were measured in systole according to the guideline [10].

Automated software for aortic measurement using 3D-TEE data

3D-TEE datasets were analyzed off-line with the “eSie-Valves™” software (Autovalve Analysis for Syngo SC2000 Prime 4.0, Siemens Healthineers) as previous described [9, 11]. In fully automated analysis, the software automatically extracted and identified aortic anatomic landmarks of an optimal single-beat (Supplementary Figure 1), and finally exported a comma-separated-values file with the content of quantitative parameters analyzed in all or the selected frames. In semi-automated analysis, observers verified the landmarks of the automated model and manually corrected them in the model from a long axis view of the 3D data showed in different long planes and a short axis view at different levels (Fig. 1, Videos 3–6). After the necessary changes, the final results were modified to sift the true anatomy. Exported parameters included the maximal diameter, minimal diameter, perimeter, and area of AA, SOV and STJ.

We calculated the average diameter by (maximal + minimal diameter)/2, perimeter-derived diameter by perimeter/π, area-derived diameter by square root of 4 × area/π. For the full-automated analysis, a manufacturer’s product manager used the software and exported the results without any manual amendments. For the semi-automated analysis, two trained echocardiographers with 10 years (MZ) and 8 years (LW) experiences recorded measurements after independent adjustments of computational landmarks at various aortic levels. All measurements were reanalyzed twice with an interval of at least 2 weeks for estimation of intra-observer and inter-observer differences.

MDCT

All MDCT examinations were performed using a dual-source scanner (SOMATOM Definition Flash with the Stellar Detector, Siemens Healthineers). A prospectively ECG-triggered scan with padding technique and absolute phase acquisition (250 ms to 400 ms of the R–R interval) was performed to minimize the radiation, though most

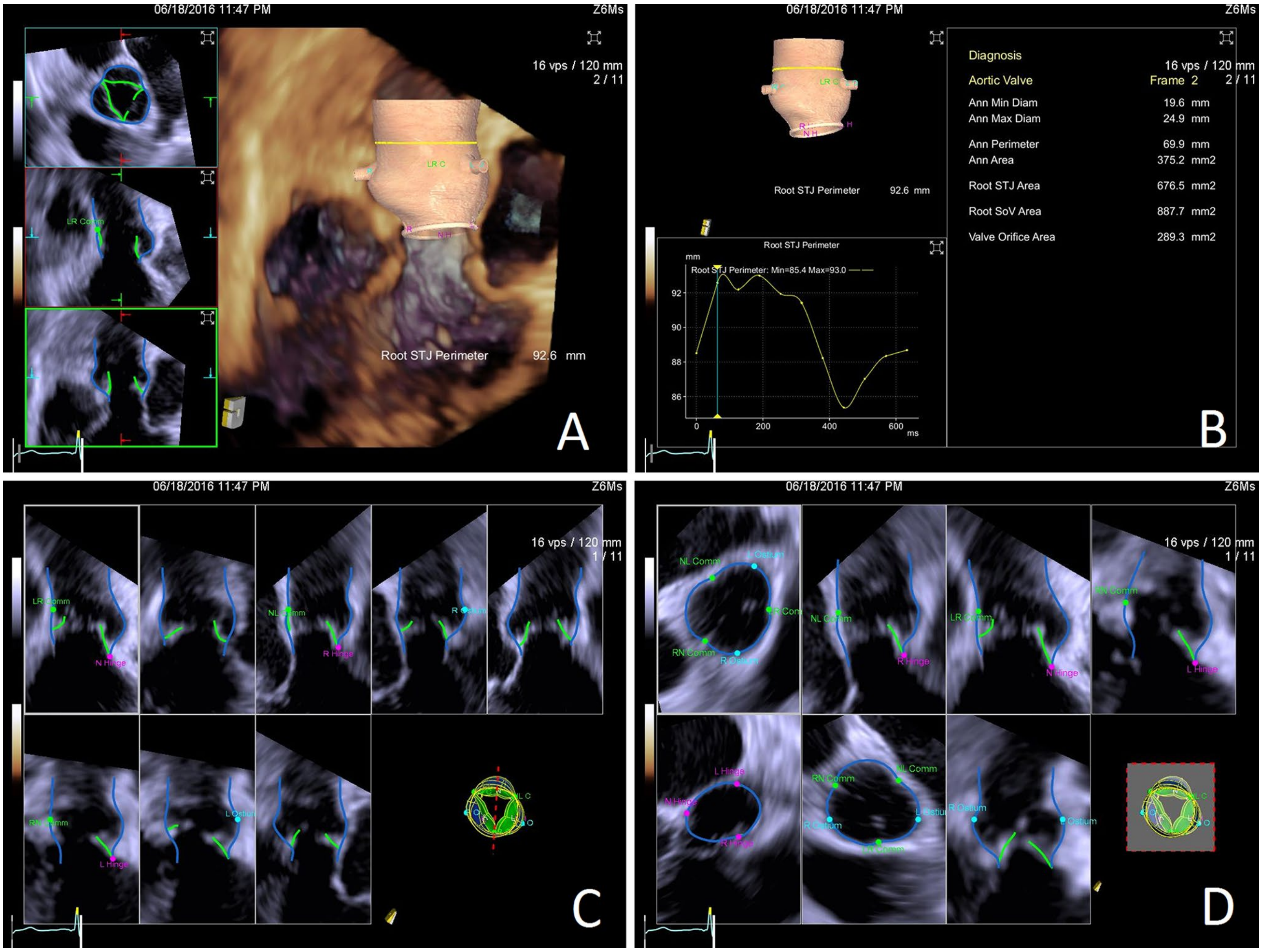

Diagnosis
Aortic Valve Frame 2
Ann Min Diam 19.6 mm
Ann Max Diam 24.9 mm
Ann Perimeter 69.9 mm
Ann Area 375.2 mm2
Root STJ Area 676.5 mm2
Root SoV Area 887.7 mm2
Valve Orifice Area 289.3 mm2

Fig. 1 Illustration of automated three-dimensional transesophageal echocardiography modeling. **a** Automatically extracting and identifying aortic anatomic landmarks in different colors: the aortic wall in blue, three leaflets in green, hinges in pink, and the coronary ostia in cyan, showing in four quadrants of the screen, the three orthogonal planes, and the full volume of the 3D dataset. **b** Exporting quantitative parameters analyzed in a whole heartbeat cycle. **c** Surface tracking of the root components in systole in the long-axis orientations and **d** in the short-axis and orthogonal long-axis orientations

candidates had atrial fibrillation [12]. Acquisition parameters and a triple-phase contrast medium injection protocol were described in detail in our previous works [13, 14]. The average radiation dose was 276.3 ± 78.5 mGy cm. All MDCT images were transferred to an external workstation (TAVR-planning module, Syngo.Via, Siemens Healthineers) and assessed by two experienced radiologists (KL and BL) independently, according to the guidelines [7]. The radiologists were blinded to echo data.

THV sizing

We chose the hypothetical prosthetic sizes according to the FDA approved criteria (Supplementary Table 1).

Statistical analysis

Statistical analyses were performed by Excel 2010 (Microsoft Corp., Redmond, WA), MedCalc version 16.8.4 (MedCalc Software, Ostend, Belgium), Prism 7 (GraphPad Software, La Jolla, CA) and SPSS Statistics 22.0 (IBM Corp., Armonk, NY). All data were first analyzed for normal distribution using the Omnibus K^2 test. For comparison of measurements by echocardiographic or MDCT methods, paired *t* test was used. Differences between methods and the reference standard were reported as bias ± levels of agreement as determined by Bland–Altman analysis. Linear correlations were analyzed and *r* values were tested. Reproducibility was assessed using (i) intraclass correlation coefficient (ICC) and (ii) Bland–Altman analysis. Fisher's exact test was used to

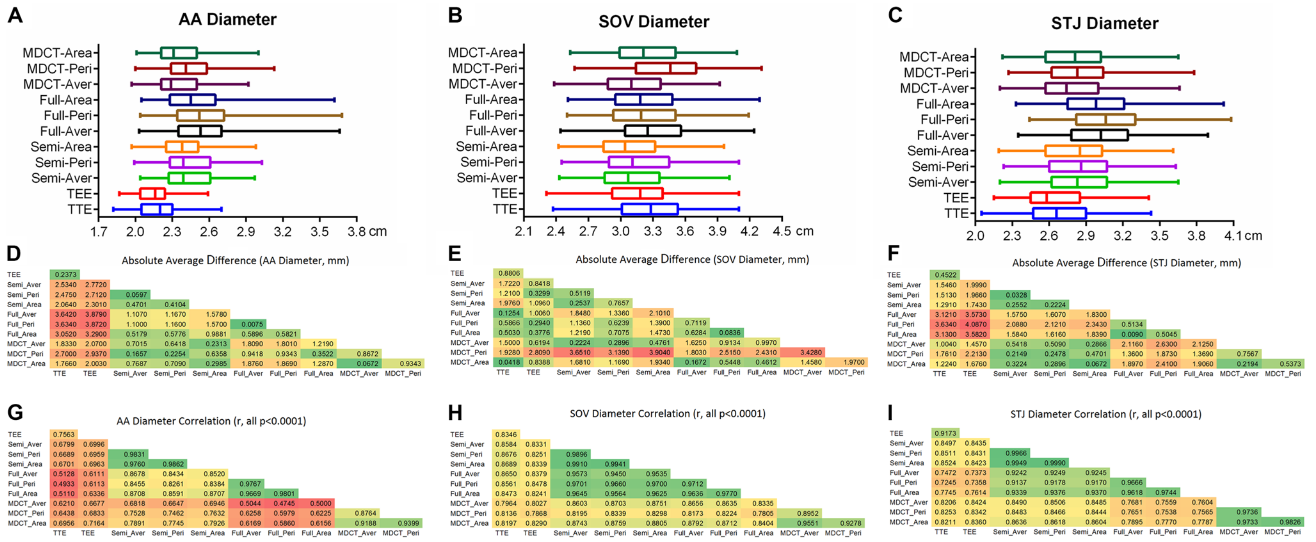

Absolute Average Difference (AA Diameter, mm)

	TTE	TEE	Semi_Aver	Semi_Peri	Semi_Area	Full_Aver	Full_Peri	Full_Area	MDCT_Aver	MDCT_Peri
TEE	0.2373									
Semi_Aver	2.5340	2.7720								
Semi_Peri	2.4750	2.7120	0.0597							
Semi_Area	2.0640	2.3010	0.4701	0.4104						
Full_Aver	3.6420	3.8790	1.1070	1.1670	1.5780					
Full_Peri	3.6340	3.8720	1.1000	1.1600	1.5700	0.0075				
Full_Area	3.0520	3.2900	0.5179	0.5776	0.9881	0.5896	0.5821			
MDCT_Aver	1.8330	2.0700	0.7015	0.6418	0.2313	1.8090	1.8010	1.2190		
MDCT_Peri	2.7000	2.9370	0.1657	0.2254	0.6358	0.9418	0.9343	0.3522	0.8672	
MDCT_Area	1.7660	2.0030	0.7687	0.7090	0.2985	1.8760	1.8690	1.2870	0.0672	0.9343

Absolute Average Difference (SOV Diameter, mm)

	TTE	TEE	Semi_Aver	Semi_Peri	Semi_Area	Full_Aver	Full_Peri	Full_Area	MDCT_Aver	MDCT_Peri
TEE	0.8806									
Semi_Aver	1.7220	0.8418								
Semi_Peri	1.2100	0.3299	0.5119							
Semi_Area	1.9760	1.0960	0.2537	0.7657						
Full_Aver	0.1254	1.0060	1.8480	1.3360	2.1010					
Full_Peri	0.5866	0.2940	1.1360	0.6239	1.3900	0.7119				
Full_Area	0.5030	0.3776	1.2190	0.7075	1.4730	0.6284	0.0836			
MDCT_Aver	1.5000	0.6194	0.2224	0.2896	0.4761	1.6250	0.9134	0.9970		
MDCT_Peri	1.9280	2.8090	3.6510	3.1390	3.9040	1.8030	2.5150	2.4310	3.4280	
MDCT_Area	0.0418	0.8388	1.6810	1.1690	1.9340	0.1672	0.5448	0.4612	1.4580	1.9700

Absolute Average Difference (STJ Diameter, mm)

	TTE	TEE	Semi_Aver	Semi_Peri	Semi_Area	Full_Aver	Full_Peri	Full_Area	MDCT_Aver	MDCT_Peri
TEE	0.4522									
Semi_Aver	1.5460	1.9990								
Semi_Peri	1.5130	1.9660	0.0328							
Semi_Area	1.2910	1.7430	0.2552	0.2224						
Full_Aver	3.1210	3.5730	1.5750	1.6070	1.8300					
Full_Peri	3.6340	4.0870	2.0880	2.1210	2.3430	0.5134				
Full_Area	3.1300	3.5820	1.5840	1.6160	1.8390	0.0090	0.5045			
MDCT_Aver	1.0040	1.4570	0.5418	0.5090	0.2866	2.1160	2.6300	2.1250		
MDCT_Peri	1.7610	2.2130	0.2149	0.2478	0.4701	1.3600	1.8730	1.3690	0.7567	
MDCT_Area	1.2240	1.6760	0.3224	0.2896	0.0672	1.8970	2.4100	1.9060	0.2194	0.5373

AA Diameter Correlation (r, all p<0.0001)

	TTE	TEE	Semi_Aver	Semi_Peri	Semi_Area	Full_Aver	Full_Peri	Full_Area	MDCT_Aver	MDCT_Peri
TEE	0.7563									
Semi_Aver	0.6799	0.6996								
Semi_Peri	0.6689	0.6959	0.9831							
Semi_Area	0.6701	0.6963	0.9760	0.9862						
Full_Aver	0.5128	0.6111	0.8678	0.8434	0.8520					
Full_Peri	0.4933	0.6113	0.8455	0.8261	0.8384	0.9767				
Full_Area	0.5110	0.6336	0.8708	0.8591	0.8707	0.9669	0.9801			
MDCT_Aver	0.6210	0.6677	0.6818	0.6647	0.6946	0.5044	0.4745	0.5000		
MDCT_Peri	0.6438	0.6833	0.7528	0.7462	0.7632	0.6258	0.5979	0.6225	0.8764	
MDCT_Area	0.6956	0.7164	0.7891	0.7745	0.7926	0.6169	0.5860	0.6156	0.9188	0.9399

SOV Diameter Correlation (r, all p<0.0001)

	TTE	TEE	Semi_Aver	Semi_Peri	Semi_Area	Full_Aver	Full_Peri	Full_Area	MDCT_Aver	MDCT_Peri
TEE	0.8346									
Semi_Aver	0.8584	0.8331								
Semi_Peri	0.8676	0.8251	0.9896							
Semi_Area	0.8689	0.8339	0.9910	0.9941						
Full_Aver	0.8650	0.8379	0.9573	0.9450	0.9535					
Full_Peri	0.8561	0.8478	0.9701	0.9660	0.9700	0.9712				
Full_Area	0.8473	0.8241	0.9645	0.9564	0.9625	0.9636	0.9770			
MDCT_Aver	0.7964	0.8027	0.8603	0.8703	0.8751	0.8656	0.8635	0.8335		
MDCT_Peri	0.8136	0.7868	0.8195	0.8339	0.8298	0.8173	0.8224	0.7805	0.8952	
MDCT_Area	0.8197	0.8290	0.8743	0.8759	0.8805	0.8792	0.8712	0.8404	0.9551	0.9278

STJ Diameter Correlation (r, all p<0.0001)

	TTE	TEE	Semi_Aver	Semi_Peri	Semi_Area	Full_Aver	Full_Peri	Full_Area	MDCT_Aver	MDCT_Peri
TEE	0.9173									
Semi_Aver	0.8497	0.8435								
Semi_Peri	0.8511	0.8431	0.9966							
Semi_Area	0.8524	0.8423	0.9949	0.9990						
Full_Aver	0.7472	0.7373	0.9242	0.9249	0.9245					
Full_Peri	0.7245	0.7358	0.9137	0.9178	0.9170	0.9666				
Full_Area	0.7745	0.7614	0.9339	0.9376	0.9370	0.9618	0.9744			
MDCT_Aver	0.8206	0.8424	0.8490	0.8506	0.8485	0.7681	0.7559	0.7604		
MDCT_Peri	0.8253	0.8342	0.8483	0.8466	0.8444	0.7651	0.7538	0.7565	0.9736	
MDCT_Area	0.8211	0.8360	0.8636	0.8618	0.8604	0.7895	0.7770	0.7787	0.9733	0.9826

Fig. 2 Box and whiskers charts (min to max), average differences, and correlations among various measurements

determine the differences of various THV sizing criterion. A *p* value ≤ 0.05 was considered significant. All data were verified by a third-party contract research organization (Beijing BestMedInfo Co., ltd.), and all analyses were verified by a biomedical statistician using SAS version 9.3 (SAS Institute, Inc., Chicago, IL).

Results

Population

Initially 77 patients were enrolled. Eight patients dequeued for abnormal aortic anatomy after TTE examinations (3 for aortic stenosis, 1 for aortic regurgitation, 3 for mitral stenosis, and 1 for aortic dilatation), and two more patients were excluded after TEE examinations (1 for partial recording, and 1 for suboptimal image quality). All MDCT images were of good diagnostic quality. Finally, 67 patients' data were analyzed (Table 1, Supplementary Table 2).

Table 1 Clinical characteristics of the study population

Participants, n	67
Male, n (%)	46 (68.7%)
Age, years (mean ± standard deviation)	53.86 ± 12.97
Age, years (median, range)	55, 18–75
Height, m	1.69 ± 0.08
Weight, kg	72.57 ± 12.26
Body mass index, kg/m^2	25.37 ± 3.26
Body surface area, m^2	1.82 ± 0.18
Smoking, n (%)	25 (37.3%)
Hypertension, n (%)	33 (49.3%)
Diabetes, n (%)	14 (20.9%)
Hyperlipidemia, n (%)	22 (32.8%)
Stroke, n (%)	9 (13.2%)
Left ventricular ejection fraction (%)	59.88 ± 4.68
Atrial fibrillation or flutter, n (%)	57 (85.1%)
Ventricular tachycardia, n (%)	1 (1.5%)
Suspected patent foramen ovale, n (%)	6 (9.0%)
Prior to atrial septal closure	3 (4.5%)

AA, SOV, and STJ diameters

The AA, SOV, and STJ diameters were assessed via 11 methods, i.e., 2D-TTE, 2D-TEE, average diameter by semi-automated 3D-TEE modeling (Semi-Aver), perimeter-derived diameter by semi-automated 3D-TEE modeling (Semi-Peri), area-derived diameter by semi-automated 3D-TEE modeling (Semi-Area), average diameter by full-automated 3D-TEE modeling (Full-Aver), perimeter-derived diameter by full-automated 3D-TEE modeling (Full-Peri), area-derived diameter by full-automated 3D-TEE modeling (Full-Area), average diameter by MDCT (MDCT-Aver), perimeter-derived diameter by MDCT (MDCT-Peri), area-derived diameter by MDCT (MDCT-Area). The AA, SOV, and STJ diameters were demonstrated in box and whiskers charts (Fig. 2a–c). The absolute average differences and linear correlations among various measurements were illustrated in staircase pattern (Fig. 2d–i, Supplementary Figures 2–5 and Supplementary Tables 3, 4).

Intra- and inter-observer variability of semi- and full-automated 3D-TEE modeling

ICCs and correlations (*r*) showed excellent intra- and inter-observer agreements for AA, SOV and STJ diameter measurements, either using the semi- or full-automated 3D-TEE modeling methods (Table 2, Supplementary Figure 6).

Hypothetical THV sizing

There were no statistical differences among TTE, TEE and MDCT sizing according to manufacturer recommended criterion for AA diameters ($p > 0.05$, Fig. 3). Interestingly, if we stratified semi-automated 3D-TEE measurements using the recommended echocardiographic criterion for SAPIEN 3 valves, we would choose more large size valves than MDCT sizing ($p < 0.0001$). The same result was found if we used

Table 2 Intra- and inter-observer variability of semi- and full-automated 3D-TEE modeling

	Semi-automated (intra-observer)			Semi-automated (inter-observer)			Full-automated		
	ICCs	95%CI	*r**	ICCs	95%CI	*r**	ICCs	95%CI	*r**
AA-Aver	0.8052	0.7013–0.8756	0.8099	0.7459	0.6171–0.8358	0.7853	0.9583	0.9331–0.9742	0.9588
AA-Peri	0.8076	0.7048–0.8772	0.8096	0.7873	0.6756–0.8637	0.7941	0.9532	0.9250–0.9710	0.9532
AA-Area	0.7936	0.6847–0.8679	0.7940	0.7564	0.6319–0.8429	0.7792	0.9402	0.9045–0.9628	0.9412
SOV-Aver	0.8642	0.7880–0.9143	0.8649	0.8056	0.7019–0.8759	0.8081	0.8935	0.8324–0.9332	0.8936
SOV-Peri	0.8898	0.8267–0.9308	0.8898	0.8316	0.7398–0.8930	0.8081	0.9419	0.9072–0.9639	0.9432
SOV-Area	0.8771	0.8075–0.9227	0.8791	0.8362	0.7465–0.8960	0.8394	0.8888	0.8252–0.9301	0.8889
STJ-Aver	0.9549	0.9276–0.9720	0.9555	0.9137	0.8633–0.9461	0.9137	0.9703	0.9521–0.9816	0.9709
STJ-Peri	0.9551	0.9280–0.9722	0.9553	0.9248	0.8805–0.9531	0.9250	0.9333	0.8937–0.9585	0.9337
STJ-Area	0.9595	0.9349–0.9749	0.9624	0.9241	0.8794–0.9527	0.9244	0.9552	0.9281–0.9722	0.9553

*All $p < 0.0001$

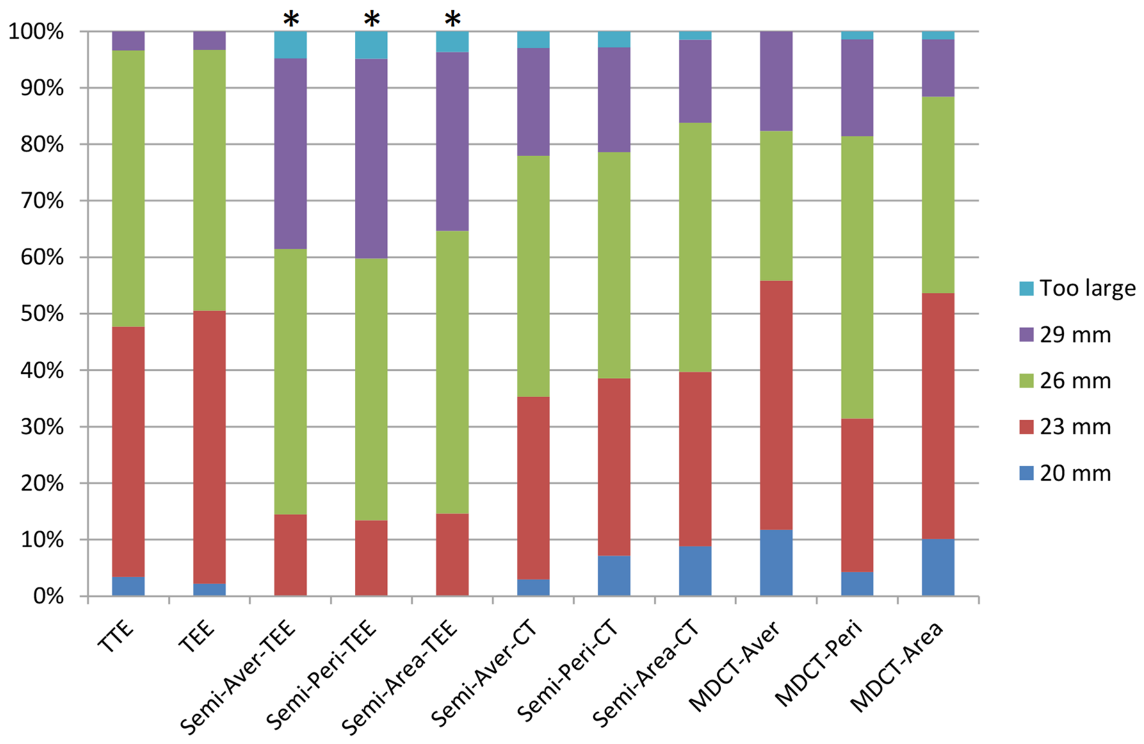

Fig. 3 Transcatheter heart valve sizing (SAPIEN 3) results by the 2D-TEE, 2D-TEE, semi-automated modeled 3D-TEE and MDCT measurements. "-TEE": according to the manufacturer recommended TEE criterion. "-CT": according to the manufacturer recommended CT criterion. $^{*}p < 0.0001$

the CoreValve sizing criterion (Supplementary Figure 7). However, if we used the recommended MDCT criterion (SAPIEN 3) instead, the sizing results would be statistically consistent with MDCT ($p > 0.05$).

Discussion

We have demonstrated, for the first head-to-head comparison, the ability of an automated algorithm to model aortic roots from 3D-TEE, comparing with conventional 2D-TTE, 2D-TEE and MDCT data. The principal findings of this study are that (i) a novel, off-line use of commercially available software allows 3D-TEE aortic root measurements (AA, SOV, STJ) to be made, which closely approximate MDCT geometry; (ii) reliability assessment of this aortic modeling algorithm indicates good reproducibility; (iii) the semi-automated 3D-TEE modeling shows more approximate results to MDCT, and the full-automated algorithm needs further optimization; (iv) THV sizing by this modeled 3D-TEE measurements is compliant with MDCT, but should use the planimetered MDCT criterion instead of conventional TEE criterion.

Accurate aortic geometry definition is of paramount importance before selecting a prosthetic aortic valve for TAVR candidates. As TAVR techniques advance, multimodality imaging of aortic dimensions develops. Even though there are large series of cases with different imaging modalities, there is no consensus regarding the ideal imaging method. In guidelines, TTE, TEE and MDCT are all imaging modalities recommended as work-up study before TAVR [3–7]. Though magnetic resonance imaging is now increasingly used in young individuals, it is not as widely available and requires longer examination time [15].

For any heart valve dysfunction, TTE is always the first-line examination. However in most patients, the aortic annulus has an oval shape. On the basis of their viewing angle, both 2D-TTE (parasternal long-axis view) and 2D-TEE (120° left ventricular outflow tract view) usually show the smaller (sagittal) diameter of aortic annulus [6]. Though 3D echocardiography has evolved greatly, its adoption is limited by (i) suboptimal temporal and spatial resolution; (ii) the erratic variability in repeated measurements. With recent advancements in electronics and miniaturization, these limitations can be overcome [16]. A handful of 3D echocardiography analysis software has been developed [9, 17, 18]. In our study, the commercial system automatically configures a geometric model of the aortic root from the images obtained by 3D-TEE and performs a quantitative analysis of these structures. This allows modeling and quantifying the aortic root from 3D-TEE data with high reproducibility. More importantly, this technique has shown good correlation with other 3D-based validated techniques, with results supporting its use in clinical practice as an alternative to MDCT prior to TAVR procedures.

Regarding 3D imaging techniques, it is generally recognized that the planimetered annular area and mean diameters are larger in systole than in diastole. Measurements of the perimeter appear to undergo a lesser degree of dynamic change throughout the cardiac cycle. However, the aortic annular area has been suggested to offer better inter-observer agreement than perimeter measurements across operators and workstation platforms [7, 19]. This is potentially due to inter-observer variability as well as a lack of standardization across workstations to generate a perimeter measurement. Many platforms lack adequate smoothing algorithms at present for hand-tracing serrated contour which results in perimeter values that are significantly larger than they are in reality [6, 7, 20]. In our study, all diameters were measured in systole, and indeed we found that the perimeter-derived diameters were larger than area-derived diameters. Among these differences between peri- and area-derived diameters, that of SOV demonstrated more apparent and that of STJ seemed subtle. The likely reason was the absolute larger diameters of SOV and the circular shape of STJ. Consequently we set the area-derived diameters from MDCT as the reference standard, also as is prosthesis valve manufacturers' recommendation.

Our results showed that modeled 3D-TEE measurements were highly correlated with the dimensions obtained from MDCT, which had been evidenced in substantial reports. A remarkable finding was the modeled 3D-TEE measurements (semi-automated) no longer yielded smaller diameters than MDCT as the previous "consensus" [21–23], but were equivalent to or even insignificantly larger than MDCT measurements. Yet we found our alliances. Tamborini reported the identical AA areas measured by 3D-TEE and MDCT (443.2 ± 97.0 mm^2 [Qlab] vs 442.5 ± 94.8 mm^2) [24]. Khalique accessed 100 TAVR candidates' aortic roots, and recorded the AA diameter of 23.6 ± 2.3 mm (Qlab) vs 23.7 ± 2.1 mm [17]. Calleja compared a cohort of normal aortic roots either accessed by 3D-TEE or MDCT, and the results were 23.3 ± 1.7 mm (Autovalve) vs 22.3 ± 2.5 mm [25]. Garcia-Martin included 10 TAVR patients, and measured the AA diameter of 22.1 ± 3.4 mm (Autovalve) vs 21.8 ± 3.1 mm [11]. These findings may be attributed to the measurements carried out by different operators and with software heavily relying on manual hand-tracing. Likewise there may be slightly systematic, methodologic reasons for the different selection of transverse planes for annulus assessment. This adds to previous evidence pointing to the imperative need of standardized protocols to accurately locate annular plane and avoid ultrasound artifacts [26, 27]. Additionally, partial acoustic shadowing of the annulus and side lobes artifacts may mislead the measurement and induce significant errors [23]. Finally, the two modalities differ in temporal resolution, and thus measurements may be performed in slightly different systolic points in the cardiac cycle.

Even though there are controversial results on 3D-TEE and MDCT measured aortic geometry, our and previous studies lead us to believe that AA diameters measured by the modeled 3D-TEE algorithm closely approximate MDCT measurements [23]. Hahn et al. [27] recommended "indirect planimetry" for 3D-TEE annular assessments. They identified the shape of the "virtual" annulus by neighboring points' consistency on the long-axis planes images, as acoustic noises were identifiable on the long-axis images and not mistaken for the annulus, which avoided the bias from direct hand-tracing on short-axis images [10]. From our user experiences, the novel 3D-TEE modeling software heavily relies on the long-axis segmentation either by full- or semi-automated manner, as following Hahn's theory [17]. We infer it as an explanation for above controversies. Besides, a competent smoothing algorithm optimizes the aortic contour, which enhances the verisimilitude.

The modeled 3D-TEE algorithm is a kind of planimetered measurements with volume rendering, as same as MDCT in nature. Therefore, we should not apply the conventional 2D echocardiographic THV sizing criterion mechanically. Our results suggested the MDCT criterion was compliant with the modeled 3D-TEE measurements. Since it was widely recognized that the TEE-measured AA diameter, including commonly used 3D-TEE, was smaller than that of MDCT, few investigators proposed a unified TAVR sizing criterion for 3D-TEE imaging before [17, 27]. Herein, we appeal for a new TAVR sizing criterion in this new echo era. Nevertheless, sizing of the aortic valve prosthesis is achieved in a multifactorial process. The implanted size is not only imaging dependent, and not relying on a single echocardiographic measurement alone, but also depends on TAVR team's experience. The discrepancy from nuanced THV sizing criterion will be neutralized, i.e. statistically meaningful but not clinically relevant.

Beside the AA diameters, the SOV and STJ diameters are of importance during TAVR procedure, especially for the self-expanding valves. All the SOV and STJ diameters of our participants conform to the requirements of commercial available self-expanding valves. Meanwhile, our results are similar to others (SOV: 30.2 ± 2.7 mm [3D-TEE] vs 33.0 ± 3.1 mm [MDCT], STJ: 25.3 ± 2.0 mm [3D-TEE] vs 26.6 ± 2.9 mm [MDCT]) [25]. These make sense in China, as the most popular TAVR valve that is officially-approved is a self-expanding valve [28].

The full-automated modeling of aortic roots ought to be the ultimate solution, as is fast and less operator-dependent. In this study, a full-automated modeling process could be finished within two minutes, but a semi-automated modeling need estimated 4–6 h in the first 20 cases and 2–3 h in the subsequent. However, accuracy is not always compatible with time-efficiency. Judged on our results, this full-automated algorithm is immature so far. Generally, the diameters measured by full-automated modeling are larger than semi-automated manner, and sometimes there will be abnormally discrete values. We believe that in the near future, a satisfactory full-automated measurement of aortic roots by 3D-TEE will be available, along with a high resolution ultrasonic probe, an optimized algorithm for blood-tissue interface segmentation and artificial intelligence technologies.

Our study does have limitations. First, the patients included are not TAVR candidates, as there are no legally approved TAVR valves that time in China, so it is unprovable whether this software could be applied to complicated TAVR cases, whose abnormal valves often cause artifacts that do not allow precise measurements. Our participants were relatively healthy and with long life expectancy. We must not choose multiphase (cine) but prospectively low-dose acquisition for MDCT. The radiation dose was ethically acceptable that lower our routine TAVR scanning [13, 14], thus the phases that were reconstructed and measured might not present the largest diameters of aortic roots [29]. Second, majority of our participants were with arrhythmia, and there might be inadequate dilation of aortic roots and insufficient opening of aortic valves due to catalectic systole of left ventricles during MDCT scanning [12]. Third, the THV sizing was not event-driven, and manufacturer recommended THV sizing criterion was somehow overlapped, so the statistical power might be discounted. Fourth, this study only represented our limited experience of a small sized single-center study. None calcified and bicuspid valves were included. The ability of the software to model the abnormal leaflet morphology still needs to be tested.

In conclusion, the new automated 3D-TEE software allows modeling and quantifying the normal aortic root from regular 3D-TEE data with high reproducibility. Measurements by the semi-automated method closely approximate and well correlate with the corresponding MDCT, thus THV sizing by this modeled 3D-TEE measurements should adopt recommended MDCT criteria but not echocardiographic criteria. The full-automated algorithm needs further optimization, and powerful machine learning in the upcoming artificial intelligence era may be the solution [30].

Acknowledgements The authors thank Dr. Chuangshi Wang (Medical Research and Biometrics Center, State Key Laboratory of Cardiovascular Diseases, National Center for Cardiovascular Diseases; 15 Fengcunxili, Beijing 102308, China) and Dr. Zhilan Zheng (Division of Ultrasound Application, Siemens Healthineers China; 7 Wangjing Zhonghuan South Road, Beijing 100102, China) for their helps.

Funding This work was supported by the Peking Union Medical College Youth Fund from the Fundamental Research Funds for the Central Universities (No. 3332015013, to MZ) and partly by the National Natural Science Foundation of China (No. 81470080, to WH).

Compliance with ethical standards

Conflict of interests The authors have no conflicts to declare.

References

1. Giannini F, Baldetti L, Gallone G et al (2018) Transcatheter valve replacement in Asia Pacific: current practice and perspectives. J Am Coll Cardiol 72:3189–3199
2. Khalique OK, Hamid NB, White JM et al (2017) Impact of methodologic differences in three-dimensional echocardiographic measurements of the aortic annulus compared with computed tomographic angiography before transcatheter aortic valve replacement. J Am Soc Echocardiogr 30:414–421
3. Leipsic JA, Blanke P, Hanley M et al (2017) ACR appropriateness criteria((R)) imaging for transcatheter aortic valve replacement. J Am Coll Radiol 14:S449–S455
4. Soon J, Pibarot P, Blanke P et al (2017) Multimodality imaging for planning and follow-up of transcatheter aortic valve replacement. Can J Cardiol 33:1110–1123
5. Bons LR, Duijnhouwer AL, Boccalini S et al (2019) Intermodality variation of aortic dimensions: how, where and when to measure the ascending aorta. Int J Cardiol 276:230–235
6. Dulgheru R, Pibarot P, Sengupta PP et al (2016) Multimodality imaging strategies for the assessment of aortic stenosis: Viewpoint of the Heart Valve Clinic International Database (HAVEC) group. Circ Cardiovasc Imaging 9:e4352
7. Blanke P, Weir-McCall JR, Achenbach S et al (2019) Computed tomography imaging in the context of transcatheter aortic valve implantation (TAVI)/transcatheter aortic valve replacement (TAVR): an expert consensus document of the Society of Cardiovascular Computed Tomography. JACC Cardiovasc Imaging 12:1–24
8. Pibarot P, Magne J, Leipsic J et al (2019) Imaging for predicting and assessing prosthesis-patient mismatch after aortic valve replacement. JACC Cardiovasc Imaging 12:149–162
9. Kato N, Shibayama K, Noguchi M et al (2018) Superiority of novel automated assessment of aortic annulus by intraoperative three-dimensional transesophageal echocardiography in patients with severe aortic stenosis: comparison with conventional cross-sectional assessment. J Cardiol 72:321–327
10. Lang RM, Badano LP, Tsang W et al (2012) EAE/ASE recommendations for image acquisition and display using three-dimensional echocardiography. J Am Soc Echocardiogr 25:3–46
11. Garcia-Martin A, Lazaro-Rivera C, Fernandez-Golfin C et al (2016) Accuracy and reproducibility of novel echocardiographic three-dimensional automated software for the assessment of the aortic root in candidates for thanscatheter aortic valve replacement. Eur Heart J Cardiovasc Imaging 17:772–778
12. Yang L, Xu L, Schoepf UJ et al (2015) Prospectively ECG-triggered sequential dual-source coronary CT angiography in patients with atrial fibrillation: influence of heart rate on image quality and evaluation of diagnostic accuracy. PLoS ONE 10:e134194
13. Wang Y, Wang M, Song G et al (2019) Optimal pre-TAVR annulus sizing in patients with bicuspid aortic valve: area-derived perimeter by CT is the best-correlated measure with intraoperative sizing. Eur Radiol 29:259–269
14. Ren X, Zhang M, Liu K et al (2016) The significance of aortic valve calcification in patients with bicuspid aortic valve disease. Int J Cardiovasc Imaging 32:471–478
15. Mayr A, Klug G, Reinstadler SJ et al (2018) Is MRI equivalent to CT in the guidance of TAVR? A pilot study. Eur Radiol 28:4625–4634
16. Mahmood F, Shernan SK (2016) Perioperative transoesophageal echocardiography: current status and future directions. Heart 102:1159–1167
17. Khalique OK, Kodali SK, Paradis JM et al (2014) Aortic annular sizing using a novel 3-dimensional echocardiographic method: use and comparison with cardiac computed tomography. Circ Cardiovasc Imaging 7:155–163
18. Prihadi EA, van Rosendael PJ, Vollema EM et al (2018) Feasibility, accuracy, and reproducibility of aortic annular and root sizing for transcatheter aortic valve replacement using novel automated three-dimensional echocardiographic software: comparison with multi-detector row computed tomography. J Am Soc Echocardiogr 31:505–514
19. Achenbach S, Delgado V, Hausleiter J et al (2012) SCCT expert consensus document on computed tomography imaging before transcatheter aortic valve implantation (TAVI)/transcatheter aortic valve replacement (TAVR). J Cardiovasc Comput Tomogr 6:366–380
20. Podlesnikar T, Delgado V (2016) Update: Cardiac Imaging (II). transcatheter aortic valve replacement: advantages and limitations of different cardiac imaging techniques. Rev Esp Cardiol (Engl Ed) 69:310–321
21. Husser O, Holzamer A, Resch M et al (2013) Prosthesis sizing for transcatheter aortic valve implantation—comparison of three dimensional transesophageal echocardiography with multislice computed tomography. Int J Cardiol 168:3431–3438
22. Ng AC, Delgado V, van der Kley F et al (2010) Comparison of aortic root dimensions and geometries before and after transcatheter aortic valve implantation by 2- and 3-dimensional transesophageal echocardiography and multislice computed tomography. Circ Cardiovasc Imaging 3:94–102
23. Vaquerizo B, Spaziano M, Alali J et al (2016) Three-dimensional echocardiography vs. computed tomography for transcatheter aortic valve replacement sizing. Eur Heart J Cardiovasc Imaging 17:15–23
24. Tamborini G, Fusini L, Muratori M et al (2014) Feasibility and accuracy of three-dimensional transthoracic echocardiography vs. multidetector computed tomography in the evaluation of aortic valve annulus in patient candidates to transcatheter aortic valve implantation. Eur Heart J Cardiovasc Imaging 15:1316–1323
25. Calleja A, Thavendiranathan P, Ionasec RI et al (2013) Automated quantitative 3-dimensional modeling of the aortic valve and root by 3-dimensional transesophageal echocardiography in normals, aortic regurgitation, and aortic stenosis: comparison to computed tomography in normals and clinical implications. Circ Cardiovasc Imaging 6:99–108
26. Zamorano J, Pardo A (2016) 3D-ECHO for TAVI: two arrows, just in case. Eur Heart J Cardiovasc Imaging 17:9–10
27. Hahn RT, Little SH, Monaghan MJ et al (2015) Recommendations for comprehensive intraprocedural echocardiographic imaging during TAVR. JACC Cardiovasc Imaging 8:261–287
28. Liao YB, Zhao ZG, Wei X et al (2017) Transcatheter aortic valve implantation with the self-expandable venus A-Valve and CoreValve devices: preliminary experiences in China. Catheter Cardiovasc Interv 89:528–533
29. Jurencak T, Turek J, Kietselaer BL et al (2015) MDCT evaluation of aortic root and aortic valve prior to TAVI. What is the optimal imaging time point in the cardiac cycle? Eur Radiol 25:1975–1983
30. Sengupta PP, Adjeroh DA (2018) Will artificial intelligence replace the human echocardiographer? Circulation 138:1639–1642